Molecular Immunology 108 (2019) 89–101

Contents lists available at ScienceDirect

Molecular Immunology

journal homepage: www.elsevier.com/locate/molimm

Modulation of antiviral immunity by the ichnovirus HdIV in *Spodoptera frugiperda*

Vincent Visconti[1], Magali Eychenne, Isabelle Darboux*

UMR 1333 INRA - Université de Montpellier Diversité, Génomes & Interactions Microorganismes-Insectes (DGIMI), 34095 Montpellier, France

ARTICLE INFO

Keywords:
Polydnavirus
Spodoptera frugiperda
Apoptosis
Antiviral defense

ABSTRACT

Polydnaviruses (PDVs) are obligatory symbionts found in thousands of endoparasitoid species and essential for successful parasitism. The two genera of PDVs, ichnovirus (IV) and bracovirus (BV), use different sets of virulence factors to ensure successful parasitization of the host. Previous studies have shown that PDVs target apoptosis, one of the innate antiviral responses in many host organisms. However, IV and BV have been shown to have opposite effects on this process. BV induces apoptosis in host cells, whereas some IV proteins have been shown to have anti-apoptotic activity. The different biological contexts in which the assays were performed may account for this difference. In this study, we evaluated the interplay between apoptosis and the ichnovirus HdIV from the parasitoid *Hyposoter didymator,* in the HdIV-infected hemocytes and fat bodies of *S. frugiperda* larvae, and in the Sf9 insect cell line challenged with HdIV. We found that HdIV induced cell death in hemocytes and fat bodies, whereas anti-apoptotic activity was observed in HdIV-infected Sf9 cells, with and without stimulation with viral PAMPs or chemical inducers. We also used an RT-qPCR approach to determine the expression profiles of a set of genes known to encode key components of the other main antiviral immune pathways described in insects. The analysis of immune gene transcription highlighted differences in antiviral responses to HdIV as a function of host cell type. However, all these antiviral pathways appeared to be neutralized by low levels of expression for the genes encoding the key components of these pathways, in all biological contexts. Finally, we investigated the effect of HdIV on the general antiviral defenses of the lepidopteran larvae in more detail, by studying the survival of *S. frugiperda* co-infected with HdIV and the entomopathogenic densovirus JcDV. Coinfected *S. frugiperda* larvae have increased resistance to JcDV at an early phase of infection, whereas HdIV effects enhance the virulence of the virus at later stages of infection. Overall, these results reveal complex interactions between HdIV and its cellular environment.

1. Introduction

Polydnaviruses (PDVs) are enveloped, double-stranded DNA (dsDNA) viruses. These endogenous particles form obligatory symbiotic associations with tens of thousands of hymenopteran endoparasitoid species attacking the larvae of agronomically important noctuid pests. The PDV family includes the ichnovirus (IV) and bracovirus (BV) taxa, which are associated with the Ichneumonidae and Braconidae families of parasitoid wasps, respectively. IVs and BVs evolved from different viral ancestors (Beliveau et al., 2015; Drezen et al., 2017; Volkoff et al., 2010), but their life cycles and modes of action display striking similarities. Both IVs and BVs persist as proviruses integrated into the wasp's chromosome and transmitted vertically to offspring. Viral particles are produced exclusively in the calyx, a particular region of the female reproductive organ, during the parasitoid pupal stage. They contain circular dsDNA molecules produced from the proviral genome by amplification, excision and circularization of the viral DNA. The viral particles are injected into the larvae of the lepidopteran host together with the parasitoid egg. The PDVs rapidly infect multiple host cells and tissues. Viral products, which have been detected within 30 min of oviposition, neutralize host immunity or manipulate development throughout the duration of parasitism, which lasts a couple of days, to promote the development of the wasp offspring (Strand and Burke, 2012).

The packaged PDV genomes sequenced to date, which are between 190 kbp and 606 kbp kb long (Dupuy et al., 2012), contain no genes encoding the necessary proteins for viral replication. The virus cannot, therefore, replicate in the host. However, it contains more than a

* Corresponding author.
E-mail addresses: vincent.visconti34@gmail.com (V. Visconti), isabelle.darboux@inra.fr (I. Darboux).
[1] Present address: MOISIBIO, Laboratoire Universitaire de Biodiversité et Ecologie Microbienne.

https://doi.org/10.1016/j.molimm.2019.02.011
Received 1 January 2019; Received in revised form 13 February 2019; Accepted 13 February 2019
Available online 20 February 2019

hundred genes encoding proteins involved in virus-host interactions, mostly organized into gene families. The two PDV genera have very different sets of virulence genes, with only two multigene families, encoding the viral ankyrins and cysteine-rich proteins, in common (Djoumad et al., 2013b; Doremus et al., 2014; Strand and Burke, 2012; Tanaka et al., 2007; Webb et al., 2006). Nevertheless, in both these genera, virulence factor expression enables the PDV to inhibit humoral and cellular immune responses in infected or parasitized host larvae.

Several major antiviral pathways have been described in insects (Agaisse and Perrimon, 2004; Brutscher et al., 2015; Choi et al., 2012; Kingsolver et al., 2013; Liu et al., 2015; McMenamin et al., 2018). The most prominent of these response pathways is RNA interference (RNAi), which involves several molecular actors, including Dicer-2 and Argonaute2 (Galiana-Arnoux et al., 2006; Gammon and Mello, 2015). The two NFkB-dependent signaling pathways based on Toll and Imd, and signal transduction through the Janus kinase/signal transducer and activator of transcription (JAK-STAT) system, the roles of which in responses to bacterial and fungal infections have been well studied, have also been implicated in antiviral immunity (Avadhanula et al., 2009; Costa et al., 2009; Dostert et al., 2005; Ferreira et al., 2014; Paradkar et al., 2012; Zambon et al., 2005). All these pathways require specific molecular factors, and many are regulated at the transcriptional level during viral infection (Liu et al., 2015). Apoptosis, a form of programmed cell death involved in normal organogenesis and tissue development, is also part of the insect response to viral infection, through the destruction of infected cells. This “cell suicide”, mediated by a cascade of proteolytic events induced by the activation of a group of proteases known as caspases, prevents the production and transmission of progeny virions to uninfected healthy cells early in infection (Clem, 2001, 2016; Feng et al., 2007; Miao et al., 2016).

Apoptosis is the most widely studied antiviral response to PDV-associated parasitism to date. BVs are potent inducers of apoptosis in hemocytes and insect cell lines, despite the lack of PDV replication in host cells (Djoumad et al., 2013a; Fath-Goodin et al., 2009; Kroemer and Webb, 2006; Li et al., 2014; Salvia et al., 2017; Strand and Pech, 1995; Suderman et al., 2008). This does not appear to be exclusively a cellular response to the presence of the virus. Instead, it seems to be an active process initiated by the virus, to eliminate immune cells involved in the encapsulation of parasite eggs. Indeed, some viral proteins have been shown to induce apoptosis when expressed in cell lines (Salvia et al., 2017; Suderman et al., 2008). Studies on the interactions between ichnoviruses and apoptosis have shown the situation to be more complex. The ichnovirus HfIV induces apoptosis in cultured Ld652Y insect cells (Kim et al., 1996). On the other hand, another ichnovirus, TrIV, regulates apoptosis differently in different cell lines (Beliveau et al., 2003; Djoumad et al., 2013a). Moreover, no ichnovirus proteins with pro-apoptotic activity have yet been identified, but two vankyrins from the ichnovirus CsIV have been shown to have anti-apoptotic activity in Sf9 cells, enhancing survival in cells infected with the baculovirus AcMNPV (Fath-Goodin et al., 2009).

Hyposoter didymator ichnovirus (HdIV) is the PDV carried by the endoparasitoid wasp *Hyposoter didymator*, which parasitizes noctuids, including the agronomically important pest insect *Spodoptera* spp. We have shown that the infection of *S. frugiperda* larvae with HdIV strongly decreases total hemocyte counts (THCs) 24 h post-infection (Provost et al., 2011). This decrease concerns both granulocytes and plasmatocytes, the two main subtypes of hemocytes in lepidopterans. The capacity of BVs to induce apoptosis in infected cells suggests that the decrease in THC may be due to the induction of apoptosis by HdIV. In this study, we evaluated the interplay between apoptosis in *S. frugiperda* cells and the ichnovirus HdIV. We analyzed apoptotic activity in hemocytes and fat bodies of *S. frugiperda* larvae, and in the insect cell line, Sf9, after infection with HdIV. We analyzed the regulation of the other antiviral pathways by HdIV, by quantifying the expression of a set of immune genes involved in antiviral defense, by RT-qPCR. Finally, we investigated the effects of HdIV on the general antiviral defenses of the lepidopteran larvae in more detail, by investigating the survival of *S. frugiperda* co-infected with HdIV and the entomopathogenic densovirus JcDV.

2. Materials and methods

2.1. Insect, virus and Sf9 cells

S. frugiperda larvae, from the corn-strain originated from French Guadeloupe and maintained in the DGIMI laboratory for many years, were reared on a semisynthetic diet (Poitout artificial diet; (Poitout and Bues, 1974)) at 25 °C, under a photoperiod of 16 h light and 8 h dark. *H. didymator* parasitoids were reared on *S. frugiperda* at 27 °C with a 16 h light: 8 h dark photoperiod. Calyx fluid containing the polydnavirus HdIV was prepared as described by (Clavijo et al., 2011). *S. frugiperda* Sf9 cells were routinely grown in suspension in serum-free Sf900 medium (Gibco) at 28 °C.

2.2. HdIV infection

Sf9 cells were used to seed 24-well dishes at a density of 4×10^5 cells/well and were infected with HdIV at a ratio of 0.01 wasp equivalents weq per 10,000 cells, unless otherwise specified. One wasp equivalent (weq) is defined as the amount of HdIV collected from the ovaries of a single adult female. The virus was allowed to adsorb to the cells for 2 h, and infected cell cultures were then washed once with Sf900 and transferred to fresh sf900 medium. The zero time point for infection was defined as the time point at which the viral inoculum was replaced with fresh Sf900 medium. We injected 0.5 weq HdIV in a final volume of 10 µl into each freshly molted fifth-instar larva (1 day old). PBS was injected into the negative control larvae.

2.3. Caspase assay

Briefly, 4×10^4 Sf9 cells were used to seed white-walled 96-well culture plates. The cells were infected with HdIV (0.02 weq/well), or left uninfected (control). After 24 h incubation, Caspase-Glo 3/7 reagent (Promega) was then added to wells and the plate were incubated at 28 °C for 30 min. Luminescence, measured in relative luminescence units (RLUs), was recorded with a TECAN Infinite 200 plate reader. Hemocytes and fat bodies were collected 24 h after the injection of HdIV into *S. frugiperda* fifth-instar larvae. The samples were washed in PBS, and then lysed in 100 µl lysis buffer (50 mM HEPES-KOH, pH7.5, 1 mM EDTA, 0.1% (w/v) CHAPS, 5 mM DTT, 10% (w/v) sucrose and 100 mM NaCl) supplemented with 1 mM Phenylmethanesulfonyl fluoride (PMSF). Cell lysates were subjected to three freeze-thaw cycles, and centrifuged at high speed to recover the supernatant containing soluble proteins. Protein concentration was determined with the Bradford assay, with BSA as the standard. Caspase activity was measured with 13 µg protein and 100 µM of the caspase substrate Ac-DEVD-AFC (Sigma Aldrich). Fluorescence (excitation at 405 nm; emission at 510 nm) was monitored every 15 min for 5 h at 25 °C with a TECAN Infinite 200 plate reader. Caspase activity values were set to 100% for mock-infected samples, and the values for infected samples were normalized against this value.

2.4. TUNEL assay

Apoptosis in hemocytes and fat bodies was detected by the TUNEL method, 24 h after HdIV infection. Hemocytes were collected in anticoagulant buffer. After centrifugation at 800 x *g*, cells were washed in 1 x PBS and fixed by incubation with 4% paraformaldehyde for 10 min at room temperature. Fat bodies were dissected in 1 x PBS, washed in 1 x PBS and immediately transferred to 4% paraformaldehyde solution for 10 min at room temperature. TUNEL (terminal deoxynucleotidyl transferase fluorescein-12-dUTP nick-end labeling) assays were

performed with the TUNEL Dead-End Fluorometric TUNEL System kit (Promega), according to the manufacturer's instructions. Nuclei were counterstained with propidium iodide (PI). Fluorescence was studied with a Zeiss AxioImager inverted microscope, using the following lasers: 488 nm for TUNEL and 632 nm for propidium iodide. Almost 200 hemocytes per sample were counted for the determination of apoptosis rates and values are expressed ± SD, for triplicate determinations. TUNEL-positive cells (stained green) were counted in six random fields per experimental condition. The apoptotic index was calculated as the percentage of hemocytes with green nuclei divided by the total number of PI-stained cells.

2.5. Trypan blue exclusion assays

Sf9 cells were used to seed six-well plates at a density of 1×10^6 cells per well and were either mock-infected or infected with HdIV (ratio 0.01weq :10 000 cells). After 2 h of incubation, the inoculum was replaced with fresh medium. Both floating cells and attached cells were harvested after 24 h of infection and mixed with a 0.2% solution of trypan blue dye (Merck). Cells were counted with a hemocytometer and cell viability was calculated as the percentage of cells displaying trypan blue exclusion divided by the total number of cells. The percent cell death was calculated as 100 minus the percentage of viable cells. Mortality is expressed as a percentage of the value for the mock-infected control. Experiments were performed in triplicate.

2.6. Induction of apoptosis with actinomycin D

A 0.5 mg/ml stock solution of actinomycin D (Merck) was prepared in dimethyl sulfoxide (DMSO). Apoptosis was induced by treating Sf9 cells with actinomycin D (0.5 µg/µl) for 5 h. Sf9 cells treated with DMSO alone were used as a control.

2.7. In vitro transcribed dsRNA and transfection

A region of the GFP gene was amplified from the pJGFPH plasmid (Bossin et al., 2003) with a pair of specific primers containing the T7 promoter at their 5'-ends (forward primer: 5'- TAATACGACTCACTATAGGGAGAGCGAGGAGCTGTTCA and reverse primer: 5'- TAATACGACTCACTATAGGGAGAGTCCATGCCGAGAGT; the T7 promoter sequence is underlined). PCR conditions were 94 °C for 3 min, followed by 30 cycles of 94 °C for 30 s, 60 °C for 30 s and 72 °C for 2 min. The amplicon was 692 bp long. dsGFP was synthesized with the T7 RiboMAXTM Express RNAi system (Promega), according to the manufacturer's instructions. For transfection experiments, Sf9 cells were used to seed 24-well plates at a density of 3.7×10^5 cells per well, and were then transfected with 50-µl dsRNA (0.5 µg, unless otherwise specified) with the assistance of Fugene (Promega), with a Fugene:dsRNA ratio of 1:8. Cells incubated with Fugene alone were used as a control.

2.8. RNA preparation

Both floating and attached Sf9 cells and hemolymph were collected and centrifuged at 800 x *g* at 4 °C. The cell pellet was then resuspended in the TRK lysis buffer of the E.Z.N.A Total RNA Kit I (OMEGA). The fat body was dissected out under a stereomicroscope, washed in PBS and placed directly in TRK buffer for disruption. Samples were then subjected to RNA extraction for expression analysis according to the kit manufacturer's instructions. Total RNA samples were treated with TURBO DNase (Ambion). The concentration of DNase-treated RNA was assessed with a NanoDrop ND-1000 spectrophotometer. Total RNA quality was estimated by electrophoresis in a 1% agarose gel.

2.9. Reverse transcription and quantitative real-time PCR

DNase-treated RNA was reverse-transcribed with SuperScript RT II (Invitrogen) and oligodT primers (Promega). The primers used for quantitative real-time PCR are listed in Table 1. Real-time quantitative PCR was performed with a LightCycler® 480 Instrument II (Roche) and SYBR Green I Master Mix (Roche). qPCR reactions were performed in a volume of 1.5 µl containing cDNA corresponding to 6 ng total RNA. Levels of mRNA were normalized relative to *S. frugiperda rpl32*. Expression relative to the control group was determined by the $2^{-\Delta\Delta Ct}$ method. The fold-change in expression was determined with REST (REST software version 2009, Qiagen) and expressed relative to the mean for the group of controls, which was arbitrarily assigned a value of 1. The program for amplification was as follows: 95 °C for 10 min, followed by 45 cycles of 95 °C for 5 s, 60 °C for 10 s and 72 °C for 15 s, with a final cycle of 95 °C for 5 s, 65 °C for 60 s and 97 °C for 15 s.

Table 1
Primer sets for qRT-PCR.

Genes	Primer forward	Primer reverse
rpl32	TACAATCGTCAAAAAGAGGACGA	AAACCATTGGGTAGCATGTGA
STAT	TGGGGCCAGTTGGCTGAGAC	GCAGGGCATCCTTGCAGAAC
dicer-2	CAAAAGGACGACAACAGGCA	TGAGGGTCGGGAACTTATGG
relish	TATGGCACCAACAAAACGAA	CGATACCACCGAACCTGACT
spatzle	ATGCAAGCACACGAACTCAG	CGTGTCAGCGTTGTATCTGC
imd	CGTGGAGTAAGGTTGGGAAA	ATGGTCAGGCCGTATCGTAG

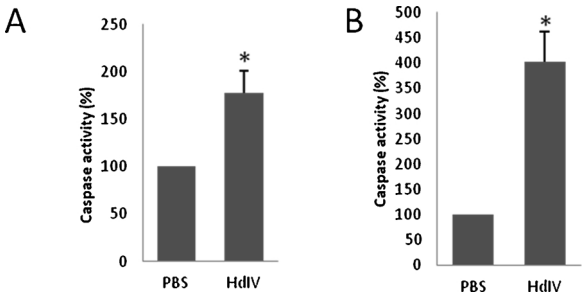

Fig. 1. HdIV induces apoptosis in the hemocytes and fat bodies of *S. frugiperda* larvae.
HdIV was injected into fifth-instar larvae of *S. frugiperda*. Hemocytes and fat bodies were recovered 24 h after infection. Caspase activity was determined in hemocytes (A) and fat bodies (B), and is expressed as a percentage relative to PBS-treated samples, the values for which were set at 100%. The results shown are means ± standard errors for four independent experiments. The statistical significance of differences was determined in Student's *t*-tests (* : $p < 0.05$).

2.10. Survival assay

Fifth-instar *S. frugiperda* larvae were infected by the injection of 10 µl of HdIV (0.5 weq/larva) or JcDV (3×10^9 viral genome equivalents/larva) with a syringe pump (KD Scientific Legato 100, Delta Labo). For the co-infection experiment, a mixture of HdIV and JcDV was prepared, such that 10 µl of this solution contained 0.5 weq of HdIV and 3×10^9 viral genome equivalents of JcDV. PBS-injected larvae were used as a mock-infected control. Following challenge, larvae were maintained individually in an incubator at 23 °C until the end of the bioassays and survival was monitored daily.

2.11. Statistical analysis

Statistical analyses were performed with the open-source R package (http://www.r-project.org/). The one-sample Wilcoxon signed rank test was used for comparisons of the treated and untreated groups, and Kruskal-Wallis analysis was performed for multiple group comparisons. The Benjamini-Hochberg procedure was used to control false discovery rate. Survival curves were plotted and analyzed by the Kaplan–Meier method and log-rank (Mantel–Cox) tests, with PRISM software. All

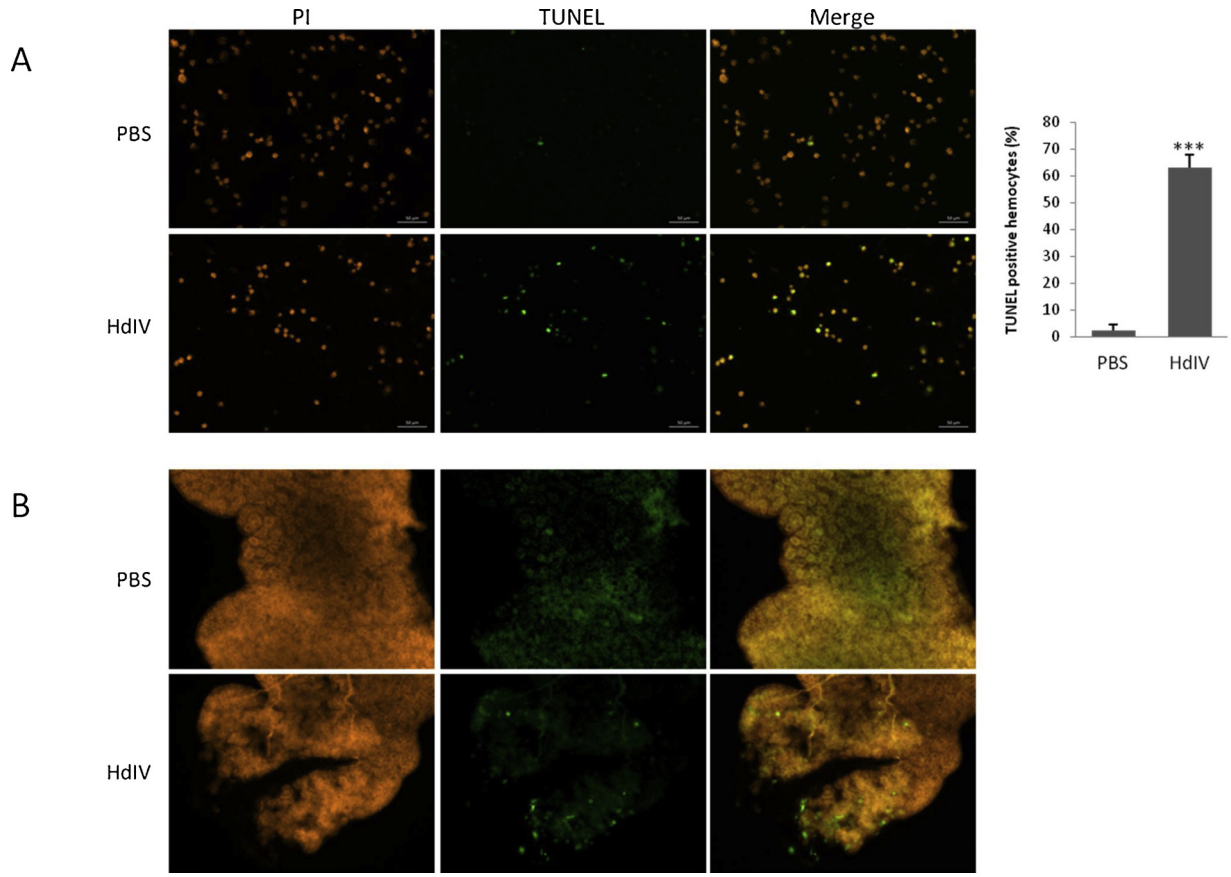

Fig. 2. TUNEL staining in hemocytes and fat bodies.
Hemocytes and fat bodies were recovered 24 h after the infection of *S. frugiperda* larvae with HdIV. Apoptotic hemocytes (A) and fat bodies (B) were stained with TUNEL reagent. Representative images are shown. The nuclei were labeled with propidium iodide (red staining) and apoptosis was detected by labeling with the TUNEL reaction mixture (green staining). The histogram shows a quantitative analysis of apoptotic hemocytes. The statistical significance of differences was determined in Student's *t*-tests (***: $p < 0.001$).

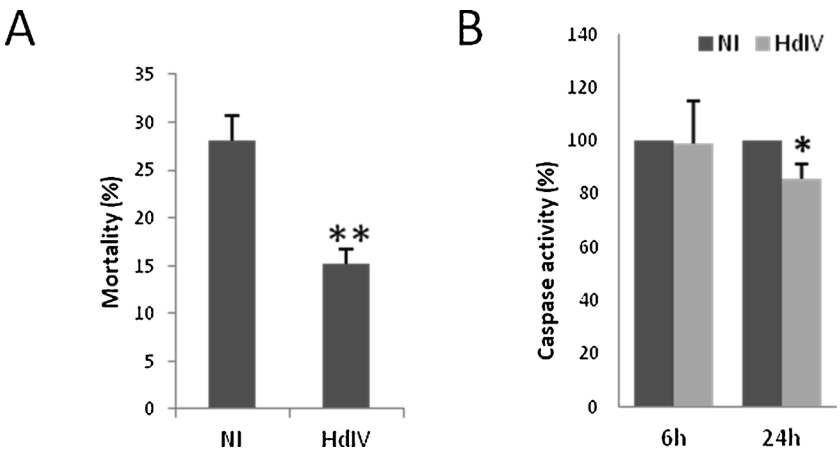

Fig. 3. HdIV enhances the survival of Sf9 cells.
(A) Sf9 cells were infected with HdIV for 24 h. Mortality was recorded by staining the cells with Trypan blue.
(B) Caspase activity was measured by assessing DEVD-AFC cleavage and is expressed as a percentage relative to control uninfected Sf9 cells (set at 100%) at each time point. The results shown are the means of 3 (for A) or 4 (for B) independent experiments and the error bars indicate standard errors. Significant differences are indicated by asterisks (* : $p < 0.05$; **: $p < 0.01$).

bioassays were performed on at least 20–36 larvae per treatment. At least three replicates were performed for each experiment. In all cases, similar results were obtained for replicate experiments.Differences were considered significant if $P < 0.05$.

3. Results

3.1. HdIV induces apoptosis in the immune cells of S. frugiperda larvae

The infection of *S. frugiperda* larvae with HdIV led to a significant decrease in total hemocyte count 24 h post-infection (p.i.) (Provost et al., 2011). We investigated whether this loss of immune cells was due to the induction of apoptosis by the virus, by infecting *S. frugiperda* larvae with HdIV and measuring caspase activity in hemocytes and fat bodies. Caspases (cysteine aspartatic proteases) play a key molecular role in apoptotic death. The activation of these proteins in response to diverse physiological and pathological stimuli led to a series of proteolytic cascades resulting in typical morphological features, such as cell shrinkage, chromatin condensation, DNA cleavage and fragmentation into membrane-bound apoptotic bodies. Caspase activity in hemocytes and fat bodies was significantly higher after HdIV infection than in mock-injected larvae (Fig. 1). TUNEL assays, which are based

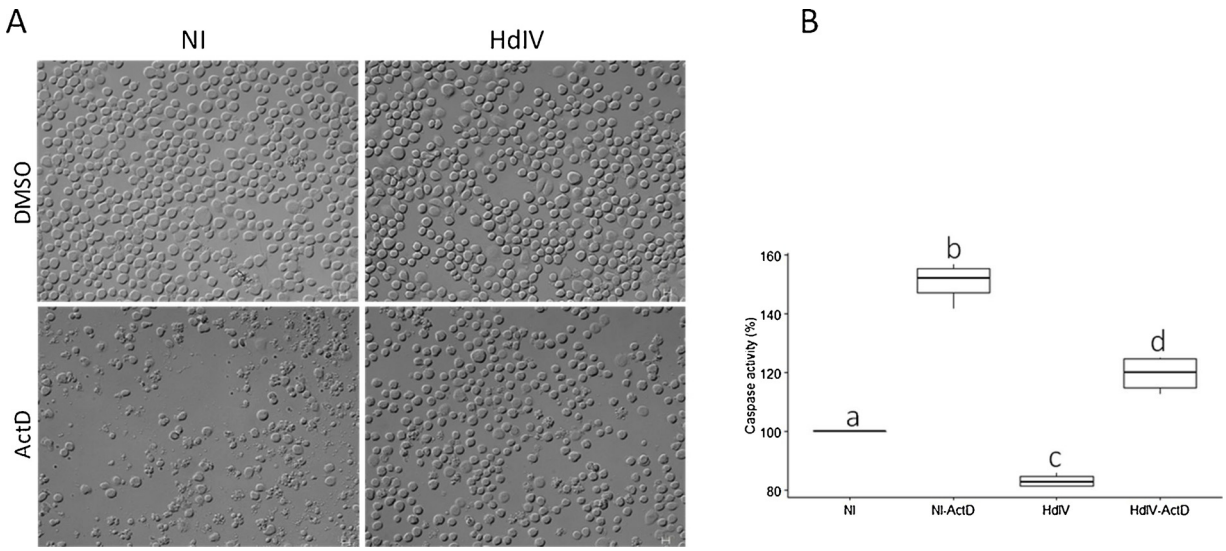

Fig. 4. HdIV reduces the apoptosis-mediated cell death induced by ActD.
Sf9 cells were left non-infected (NI) or were infected with HdIV for 19 h before treatment with the inducer of apoptosis ActD (500 ng/ml) or with DMSO (vehicle control) for 5 h. (A) Micrograph of cells showing that the treatment of uninfected cells with ActD led to a clear membrane blebbing phenotype, a common morphological feature of apoptotic cell death. By contrast, far fewer cells HdIV-infected cells displayed this phenomenon. (B) Caspase activity was measured with a luminogenic substrate, DEVD, and is expressed as a percentage relative to uninfected Sf9 cells treated with vehicle (DMSO) alone (set at 100%). Box plots marked with the same letters are not significantly different ($p < 0.05$ considered significant).

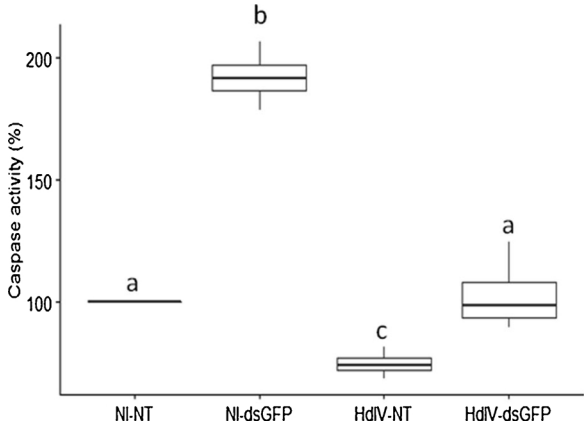

Fig. 5. Survival is higher in HdIV-infected Sf9 cells than in uninfected cells following the induction of apoptosis by double-stranded RNA.
Sf9 cells were mock-infected or infected with HdIV for 19 h and transfected with dsGFP for 5 h. Caspase activity was measured by assessing DEVD-AFC cleavage and is expressed as a percentage relative to uninfected Sf9 cells treated with the transfectant FUGENE alone. Box plots marked with the same letters are not significantly different ($P < 0.05$ considered significant).

on the staining of fragmented DNA ends, were performed to confirm that this enzyme induction was related to apoptosis. Fluorescence microscopy revealed TUNEL-positive cells in both hemocytes and fat body samples (Fig. 2).

3.2. HdIV infection inhibits induction of apoptosis in Sf9 cells

The Sf9 insect cell line, derived from *S. frugiperda* ovaries, was infected with HdIV, and cell survival was evaluated by trypan blue staining after 24 h. Mortality rates were significantly lower in infected Sf9 cells than in uninfected control cells (Fig. 3A). Increasing the dose of HdIV or the infection time had no effect on mortality (data not shown). Indeed, we detected the expression of viral genes for up to five weeks after initial infection, suggesting that infected cells could be maintained in culture without any clearly deleterious effect (data not shown). This finding led us to investigate whether HdIV had anti-apoptotic activity in Sf9 cells. We tested this hypothesis, by infecting Sf9 cells with HdIV and measuring caspase activity 6 h and 24 h post-infection (p.i.). By 6 h p.i., caspase levels were similar to those in control cells. By contrast, at 24 h, apoptotic activity was significantly lower in HdIV-infected Sf9 cells than in uninfected cells (Fig. 3B).

We evaluated the capacity of HdIV to downregulate apoptosis further, by infecting Sf9 cells with HdIV for 19 h or leaving them uninfected and then treating them with actinomycin D (ActD) for 5 h. ActD causes single-stranded breaks in DNA and inhibits RNA synthesis, thereby inducing apoptosis in Sf9 cells (Kumarswamy and Chandna, 2010). Microscopy revealed that uninfected cells treated with ActD displayed extensive membrane blebbing, a phenotype typically observed in apoptotic cells. By contrast, HdIV infection was not accompanied by such morphological changes, suggesting that the virus was able to counteract ActD-induced apoptosis (Fig. 4A). We then measured caspase activity in Sf9 cells subjected to the experimental conditions described above. Treatment with ActD clearly increased caspase activity in both uninfected and HdIV-infected cells relative to treatment with the vehicle DMSO. However, the levels of caspase activity observed in HdIV-infected Sf9 cells treated with ActD remained significantly lower than those in ActD-treated uninfected cells. These data suggest that HdIV increases the resistance of Sf9 cells to ActD-mediated apoptosis.

3.3. HdIV modulates the apoptosis induced by double-stranded RNA

We then investigated whether the virus could also block cell death induced by viral stimulation. We used foreign double-stranded RNA (dsRNA), a universal viral pathogen-associated molecular pattern (PAMP). Intracellular dsRNA is recognized by cells as a by-product of viral replication, transcription or from the secondary structures of viral RNAs. It triggers a strong sequence-independent innate antiviral response in many organisms and activates apoptosis in mammalian and invertebrate cells (DeWitte-Orr et al., 2009; Estornes et al., 2012; Flenniken and Andino, 2013; Gantier and Williams, 2007; Jacobs and Langland, 1996; Robalino et al., 2004; Wang et al., 2015; Weber et al., 2006). Indeed, 24 h after the introduction of green fluorescent protein-derived dsRNA (dsGFP) into uninfected or HdIV-infected Sf9 cells by transfection, we observed an increase in caspase activity (Fig. 5).

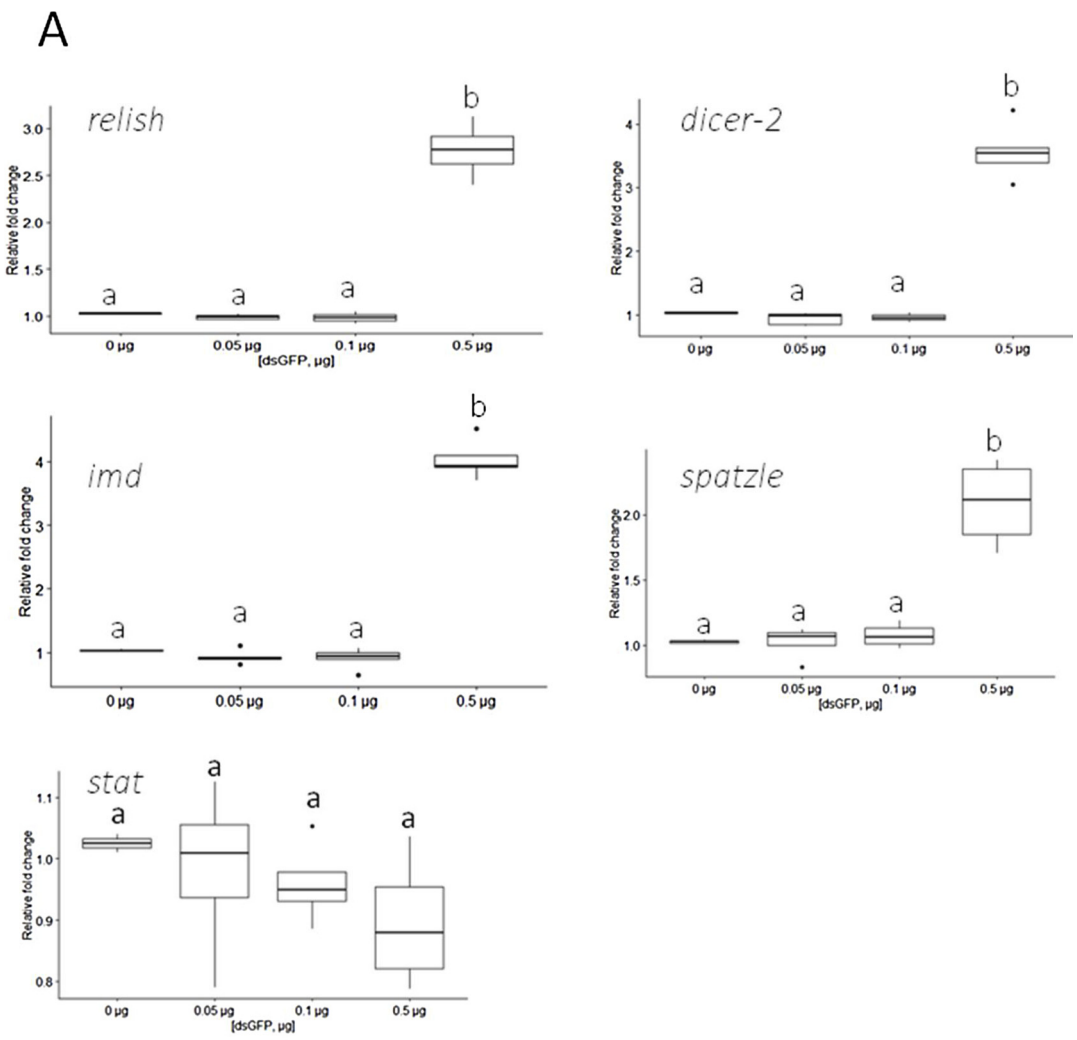

(caption on next page)

Fig. 6. Activation of antiviral gene transcription following the stimulation of Sf9 cells with a viral PAMP.
(A) Sf9 cells were transfected with three different amounts of dsGFP for 6 h. The levels of mRNA for the selected antiviral genes were quantified by RT-qPCR. Relative expression levels were calculated for each antiviral gene as a fold-change relative to the value obtained for untransfected Sf9 cells (0 µg), which was set at 1. The significance of differences between groups was assessed by Kruskal-Wallis tests with Benjamini & Hochberg correction. Box plots with different letters were considered significantly different. (B) Sf9 were transfected with 0.5 µg dsGFP for 24 h and the levels of mRNA for the selected genes were measured by RT-qPCR. Relative expression levels were calculated for each gene as a fold-change relative to the value obtained for control Sf9 cells (transfectant alone), which was set at 1. The significance of differences in expression between uninfected and HdIV-infected conditions was assessed with Wilcoxon tests. Box plots marked with an asterisk were considered significantly different (*: $p < 0.05$). In (A) and (B), transcript levels were normalized relative to the level of *rpl32* transcripts.

However, the increase in caspase activity induced by intracellular dsGFP in HdIV-infected Sf9 cells was significantly smaller than that induced in uninfected cells. This result suggests that HdIV can limit the induction of apoptosis by viral stimulation.

3.4. Transcriptional activation of the major antiviral pathways in response to a universal viral PAMP in Sf9 cells

Antiviral pathways other than apoptosis, including the RNAi, Toll, Imd and JAK/STAT pathways, have been described in insects (Cao et al., 2015; Marques and Imler, 2016). We investigated whether an RT-qPCR approach could be used to detect the induction of these defense responses after antiviral stimulation. We selected a set of genes known to be involved in antiviral defense in insects and analyzed changes in their level of expression following viral stimulation in Sf9 cells. We used double-stranded RNA (dsRNA) to mimic viral infection and trigger the antiviral response, as the use of this molecule has the advantage of limiting the risk of the transcriptional response measured being specific to a particular virus, as described in previous studies (Kemp et al., 2013). Sf9 cells were transfected with various amounts of dsGFP and the expression of *relish* and *spätzle (spzl)* from the Toll pathway, *Imd* from the IMD pathway, *dicer-2* from the RNA interference process and *stat* from the JAK/STAT pathway, was monitored by RT-qPCR, 6 h after transfection (Fig. 6A). We found that only the highest dose (0.5 µg) of intracellular dsGFP used in this experiment significantly increased the expression of almost all the selected genes, with the exception of *stat*, which remained unaffected regardless of the amount of dsGFP. An upregulation of immune genes by 0.5 µg dsGFP was also observed 24 h post-transfection, although it was weaker at this time point than at 6 h post-transfection (Fig. 6B), demonstrating the maintenance of the antiviral response over time. However, by this time point, the level of STAT expression had significantly decreased. Overall, these results demonstrate that the induction of the antiviral Toll, IMD and RNAi pathways can be detected by measuring the level of expression of selected antiviral genes, 6 h or 24 h after the application of a viral PAMP, provided that the immune stimulus is strong enough.

3.5. HdIV infection modulates the antiviral pathways differentially in S. frugiperda cells

Sf9 cells were challenged with various amounts of HdIV, and the activation of antiviral gene expression was measured by RT-qPCR, 24 h post-infection. RT-qPCR showed no upregulation of expression for any of the antiviral markers in HdIV-infected cells relative to mock-infected Sf9 cells, regardless of the amount of HdIV used. Instead, a statistically significant dose-dependent decrease in the expression of the antiviral genes was observed (Fig. 7A). We also analyzed RNA levels for the antiviral genes 6 h and 48 h after the infection of Sf9 cells with the highest dose of HdIV (Fig. 7B). Early in infection, HdIV had no effect on the transcriptional response of the cells, whereas, by 48 h after infection, a downregulation of *relish*, *spatzle* and *dicer-2*, was observed (Fig. 7B). In addition, a small but significant increase in the expression of *imd* and STAT was observed. Overall, these data show that HdIV causes an overall inhibition of the antiviral response in Sf9 cells.

We then measured the capacity of HdIV to counteract the transcriptional activation of antiviral genes in Sf9 cells stimulated with intracellular dsRNA. We infected Sf9 cells with HdIV or left them uninfected for 19 h and then transfected them with dsGFP for 6 h. RT-qPCR analysis indicated that intracellular dsGFP induced the expression of all the antiviral genes in both uninfected and HdIV-infected cells (Fig. 8). The levels of *relish* and *imd* expression were similar to those observed in uninfected Sf9 cells treated with dsGFP. However, the induction of *spatzle* and *dicer-2* was significantly weaker in HdIV-infected cells than in uninfected Sf9 cells. The presence of HdIV or intracellular dsRNA had no effect on STAT expression. These results suggest that HdIV may impair the activation of the antiviral response mediated by the Toll and RNAi pathways in Sf9 cells subjected to viral stimulation.

We investigated the potential of HdIV to regulate the transcription of antiviral genes *in vivo*, by performing RT-qPCR to evaluate the expression of these genes in hemocytes and fat bodies, 24 h after infection. In HdIV-infected hemocytes, the levels of mRNA for antiviral genes were similar to those in uninfected cells, except for *imd* and *dicer-2*, for which mRNA levels were significantly lower (Fig. 9). HdIV-induced transcriptional regulation was stronger in the fat body than in hemocytes. HdIV inhibited the expression of *spatzle*, *dicer-2* and *stat*, but significantly increased the expression of *relish* and *imd* (Fig. 9). These results suggest that HdIV downregulates the IMD and RNAi pathways in hemocytes. In fat bodies, the Toll and RNAi pathways were inhibited, whereas the IMD pathway was induced. These data suggest that HdIV regulates antiviral defense differently in *S. frugiperda* larvae according to the biological context.

3.6. Effect of HdIV infection on viral pathogenesis during a secondary infection

We then investigated whether the regulation of antiviral immunity by HdIV affected the pathogenic outcome of infection with an entomopathogenic virus. We co-infected *S. frugiperda* with HdIV and JcDV (*Junonia coania* densovirus), a non-enveloped single-stranded DNA virus from the ambidensovirus family (Mutuel et al., 2010). *S. frugiperda* larvae infected with JcDV began to die three days after injection, and almost all the larvae died within seven days (Fig. 10). HdIV-infected larvae were small and had delayed development. However, none of the larvae died during the seven days of observation. In *S. frugiperda* larvae co-infected with JcDV and HdIV, death remained lower than in larvae infected with JcDV alone, until the fifth day (p-value < 0.0001). However, after this time point, mortality was higher than that of larvae infected with JcDV alone. All the JcDV-HdIV co-infected larvae died within seven days of infection. These findings suggest that at an early phase of HdIV infection counteracts the pathogenic effects of the entomopathogenic virus, whereas HdIV effects enhance the virulence of the virus at later stages of infection.

4. Discussion

In this study, we analyzed the regulation of the major antiviral pathways by HdIV in different biological contexts, in the hemocytes and fat bodies of *S. frugiperda* larvae and in Sf9 cells. The Sf9 cell line provides an ideal system for studying the differential regulation of antiviral responses against a particular virus. Indeed, all the major antiviral responses characterized in insects have been shown to function in this cellular environment.

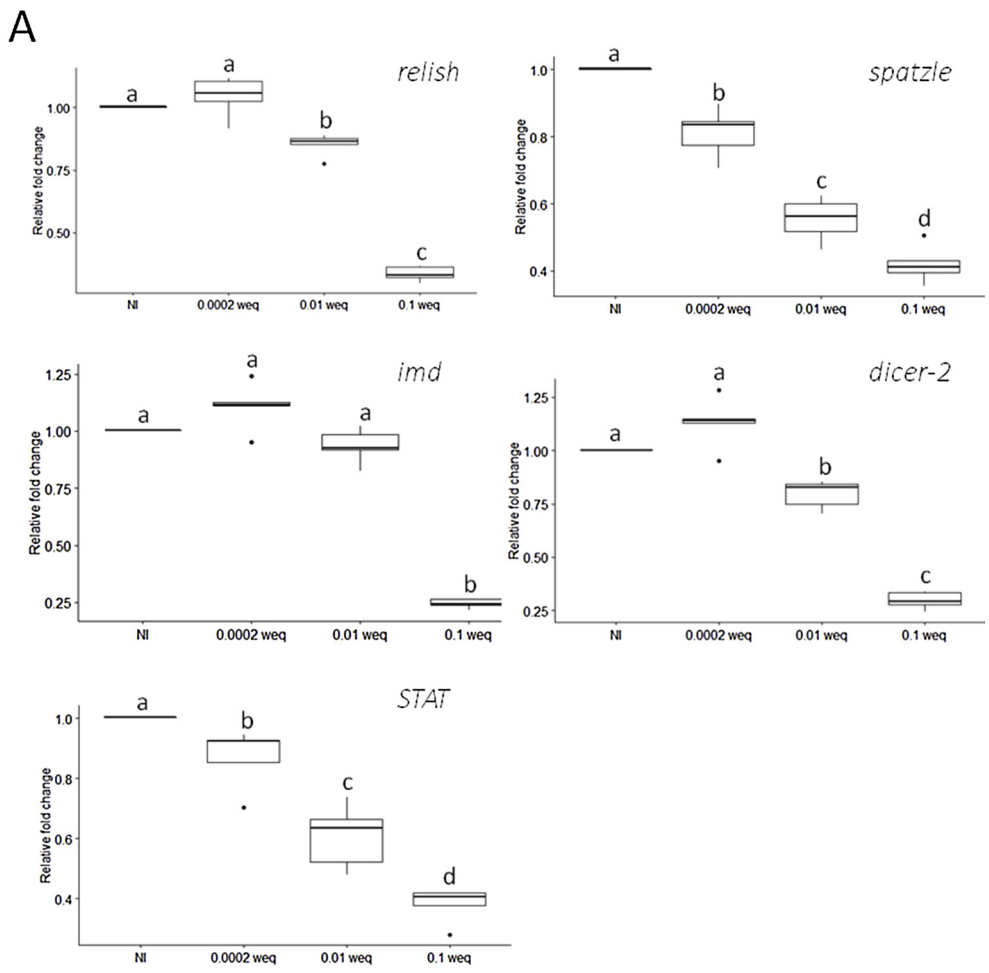

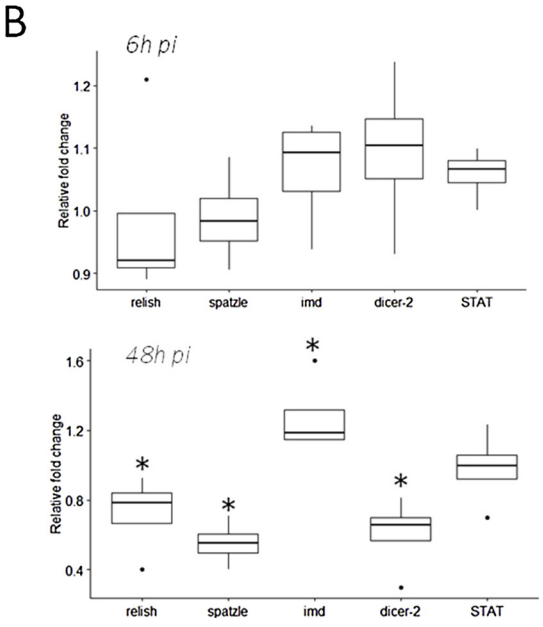

Fig. 7. Transcription levels of antiviral genes in HdIV-infected Sf9 cells.
Sf9 cells were infected with three different ratios (weq/10,000 Sf9 cells) of HdIV for 24 h. Antiviral gene expression was assessed by RT-qPCR. Data were normalized relative to *rpl32* and the normalized values for uninfected Sf9 cells (NI) were set at 1. Fold-change expression was calculated relative to NI samples. The significance of differences between groups was assessed with Kruskal-Wallis tests with Benjamini & Hochberg correction. Box plots with different letters were considered significantly different ($p < 0.05$).
(B) Sf9 cells were infected with HdIV, using a ratio of 0.01 weq per 10,000 cells, for 6 h or 48 h and the mRNA levels for the studied genes were evaluated by RT-qPCR. Data were normalized relative to *rpl32* and the normalized values for genes in uninfected Sf9 cells were set at 1. The fold-change in expression was calculated relative to control mock-infected Sf9 cells. The significance of differences between uninfected and HdIV-infected conditions was assessed with Wilcoxon tests. Box plots marked with asterisks were considered significantly different (*: $p < 0.05$).

We first focused on the apoptosis-mediated antiviral response, as a comparative analysis revealed differences in the regulation of this process by the two PDV genera. Several studies have reported the induction of apoptosis in hemocytes or cultured insect cells infected with various model BVs. *Microplitis demolitor* bracovirus (MdBV) induces apoptosis in granulocytes, one of the primary classes of hemocytes involved in the encapsulation of foreign bodies, in *Pseudoplusia includens* and *S. frugiperda* (Strand and Pech, 1995; Suderman et al., 2008). The

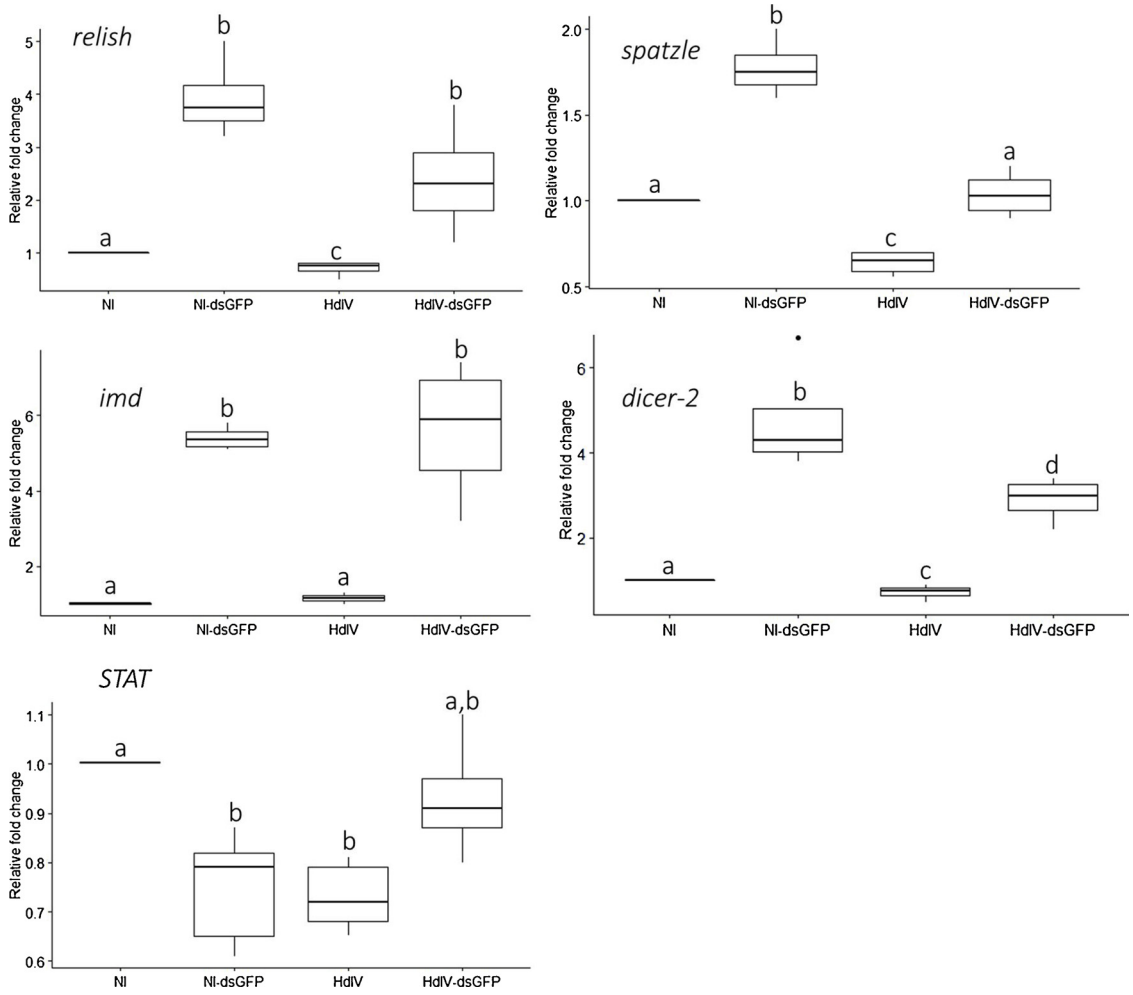

Fig. 8. Regulation of the transcription of antiviral genes in HdIV-infected Sf9 cells stimulated with dsRNA.
Sf9 cells were infected with HdIV for 19 h (HdIV) or left uninfected (NI) and were then transfected with 0.5 μg dsGFP for 6 h (HdIV-dsGFP, NI-dsGFP). The levels of mRNA for antiviral genes were then assessed by RT-qPCR. Data were normalized relative to *rpl32* and the normalized values for antiviral genes in NI conditions were set at 1. The fold-change in expression was calculated relative to NI conditions. The significance of differences between groups was assessed with a Kruskal-Wallis test with Benjamini & Hochberg correction. Box plots with different letters were considered significantly different ($p < 0.05$).

protein tyrosine phosphatase PTP-H2 from MdBV can participate in this pro-apoptotic activity, since the viral protein has been shown to induce apoptosis in Sf21 cells (Suderman et al., 2008). *Microplitis bicoloratus* BV (MbBV) has also been shown to induce apoptosis in *S. litura* hemocytes (Luo and Pang, 2006). An inhibition of the expression of the translation initiation factor eIF4 A by MbBV was proposed as the molecular mechanism responsible for this effect (Dong et al., 2017). In another hand, a transcriptomic analysis showed that the induction of apoptosis observed in *S. litura* hemocytes was due to the activation of several apoptotic caspase-dependent and caspase-independent signaling pathways (Li et al., 2014). It has been shown in another BV model that the expression of TnBV1 from *Toxoneuron nigriceps* BV (TnBV) induces high levels of mortality in lepidopteran cell lines, together with features reminiscent of apoptosis (Lapointe et al., 2007). Another TnBV protein, TnBVank1, from the vankyrin family, has also been shown to display pro-apoptotic activity when expressed in *Drosophila* S2 cells or in *H. virescens* hemocytes transfected with the *TnBVank1* gene (Salvia et al., 2017). Biochemical experiments have identified at least two cellular targets of TnBVank1, one corresponding to the transcription nuclear factor κB (NF-κB), and the other to an ALG-2-interacting protein X (Alix/AIP1) interacting with apoptosis-linked gene protein 2 (ALG-2) (Salvia et al., 2017). The expression of BV products with apoptosis-inducing activity suggests that the induction of apoptosis by BV is more than just a defense mechanism activated by the host to eliminate infected cells and preventing spreading of the pathogen. Instead, this suggests an active process deliberately used by the virus to eliminate the immune cells, which might otherwise destroy the progeny of the parasitoid. The regulation of apoptosis by IVs has been much less studied. Kroemer and Webb demonstrated that some proteins of the vankyrin family from *Campoletis sonorensis* ichnovirus (CsIV) displaying similarities to the ankyrin repeat domains of insect and mammalian IκB factors prevented the death and lysis of Sf9 cells infected with the baculovirus AcMNPV, suggesting that these viral proteins have anti-apoptotic properties (Kroemer and Webb, 2006). Indeed, this hypothesis was confirmed for one of these vankyrins, which may inhibit the NF-κB transcription factor in Sf9 cells (Fath-Goodin et al., 2009). By contrast, one study reported that cultured *Choristoneura fumiferana* cells displayed cytopathic alterations characteristics of apoptosis following infection with the PDV *Tranosema rostrale* ichnovirus (TrIV) (Beliveau et al., 2003).

We show here that HdIV induces apoptosis in the fat body and hemocytes of *S. frugiperda*. This finding is consistent with the significant decrease in THC previously reported in HdIV-infected larvae 24 h p.i. (Provost et al., 2011). As the decrease in THC affects both granulocytes and plasmocytes, apoptosis is probably activated in both these types of hemocytes, rather than in granulocytes alone, as reported for BV. The induction of apoptosis in HdIV-infected fat bodies is also consistent with the decrease in the mass and volume of tissue observed in the

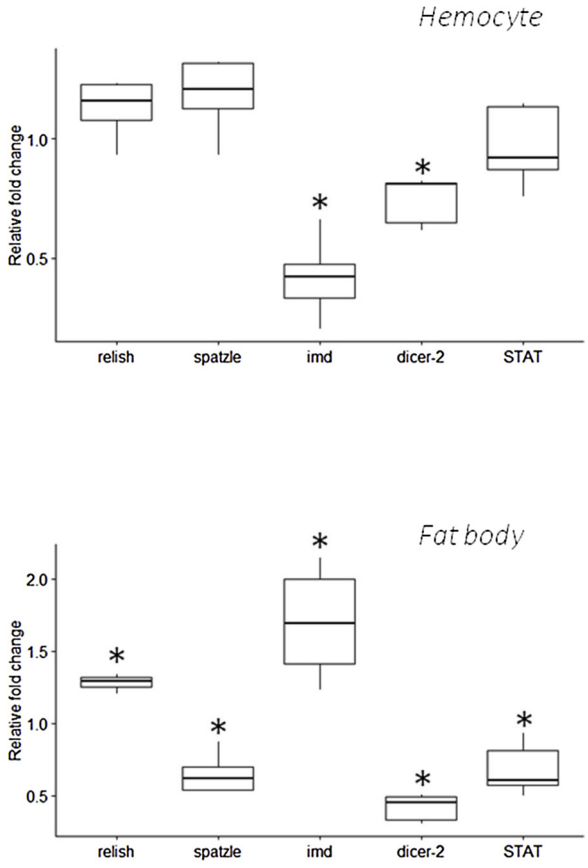

Fig. 9. Regulation of antiviral pathways in HdIV-infected *S. frugiperda* larvae. HdIV was injected into *S. frugiperda* larvae. Total RNA was isolated from hemocytes or fat bodies 24 h after injection and the mRNA levels for antiviral genes were analyzed by RT-qPCR. Data were normalized relative to *rpl32*. The normalized values for antiviral genes in uninfected samples were set at 1 and the fold-change in expression was calculated relative to control mock-infected samples. Significant differences are indicated by asterisks (*: $p < 0.05$).

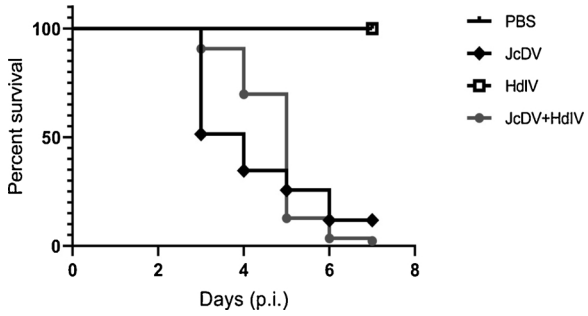

Fig. 10. HdIV modulated the susceptibility of *S. frugiperda* larvae to infection by the densovirus JcDV. Larvae were infected by an injection of HdIV, JcDV or a mixture of HdIV and JcDV. Control larvae received injections of PBS. Survival was monitored daily for seven days. None of the mock-infected or HdIV-infected larvae died during the period of analysis. JcDV-infected larvae had a significant decrease in survival when compared to JcDV-HdIV co-infected larvae until the fifth day ($p < 0.0001$). Survival bioassays data from three independent experiments, each including at least 20 larvae, are shown. P-value was calculated using Log-rank test.

course of HdIV infection (Darboux, unpublished results). By contrast, anti-apoptotic activity was observed in HdIV-infected Sf9 cells, even when these cells were challenged with different apoptotic inducers, including dsRNA, ActD and camptothecin (data not shown). The mechanisms of action of these molecules are different, suggesting that HdIV targets a step common to the different apoptotic pathways activated by these molecules. This anti-apoptotic phenotype observed in Sf9 cells raises the question as to whether this property is an artifact of cultured cells, which have adapted and proliferate indefinitely in favorable medium. However, we can rule out this hypothesis, as BVs are able to induce apoptosis in this cell line. It therefore appears more likely that the anti-apoptotic effect observed in Sf9 cells reflects an as yet unidentified activity induced in a set of tissues or cells. The midgut is a possible candidate for involvement in this process. Indeed, during normal metamorphosis, the insect midgut tissue undergoes extensive remodeling. Programmed cell death plays an active role in this process, removing obsolete larval tissues (Vilaplana et al., 2007). In the absence of midgut cell death, metamorphosis is delayed (Cai et al., 2012). PDVs trigger various molecular mechanisms to arrest development and inhibit host molting, as these effects are beneficial for parasitoid development (Pruijssers et al., 2009). By hampering development, the inhibition of midgut cell apoptosis may be advantageous for PDV-mediated parasitism. From the polydnavirus standpoint, there can also be benefits to block apoptosis in a subset of cells. Indeed, several studies have demonstrated the integration of PDV circles in the genome of the parasitized hosts (Beck et al., 2011; Chevignon et al., 2018; Gundersen-Rindal and Lynn, 2003; Volkoff et al., 2001). Persistence of these circles have thought to be an asset for the expression of viral products during the course of parasitism (i.e over several days), particularly in the absence of virus replication. In this context, inhibition of apoptosis may be of particular relevance for establishing persistent infections within some infected cells. Some viruses have developed such a strategy. For exemple, in mammals, the accessory protein X of Borna disease virus promotes virus persistence by preventing cell death (Poenisch et al., 2009).

The other major innate immune pathways, involving RNAi, Toll, IMD and JAK/STAT, have been shown to make virus-specific contributions to defense against invading pathogens. For example, the Toll and JAK/STAT pathways are required for the host response to the flavivirus dengue (DENV) in *Aedes aegypti*, whereas the JAK/STAT pathway restricts West Nile virus (WNV) infection in a *Culex* cell line (Paradkar et al., 2012; Souza-Neto et al., 2009; Xi et al., 2008). We used an RT-qPCR approach to analyze the regulation of all these antiviral pathways by HdIV, focusing on the expression of a set of immune genes in the presence and absence of stimulation of the antiviral response with the generic viral PAMP dsRNA. Most studies have used synthetic polyinosinic acid:polycytidylic acid (poly(I:C)) to stimulate the antiviral response of host cells. However, these molecules may introduce a bias into the analysis of antiviral responses (Gantier and Williams, 2007). We therefore preferred to use dsRNA to activate the innate immune response in Sf9 cells in this study. DsRNA acts as a general viral PAMP in many organisms and its presence, generally at high abundance, in virus-infected cells has been shown to trigger a strong, sequence-independent, antiviral state involving almost all the antiviral pathways, and ending in the death of the infected cells. Intracellular dsRNA also induces the transcription of antiviral genes. For example, the ribonuclease gene *dicer-2*, one of the two RNAi core machinery genes, is upregulated following the injection of dsRNA in *Manduca sexta* (Garbutt and Reynolds, 2012).

We found that RNAi was downregulated in all biological contexts tested (i.e hemocytes, fat bodies and Sf9 cells infected with HdIV). RNAi is a process stimulated by long dsRNA molecules, generally produced by RNA viruses during replication. However, dsRNAs may also be generated by DNA viruses as a by-product of symmetric transcription, or as a result of the formation of secondary structures in transcripts (Wang et al., 2015). Like DNA viruses, PDVs may generate these molecules during viral gene transcription, triggering the RNAi pathway. The production of miRNAs derived from the *Cotesia vestalis* bracovirus (CvBV) has recently been demonstrated in *Plutella xylostella* hosts parasitized by *C. vestalis* (Wang et al., 2018). However, to our knowledge, there is no evidence of production of viral siRNAs in insect cells infected with a PDV. The downregulation of the key gene *dicer-2*

suggests that the RNAi mechanism, along with apoptosis, is one of the primary antiviral responses targeting by HdIV. However, we cannot rule out the possibility that other mechanisms, such as the expression of viral proteins with suppressors of RNAs (VSR) activity, is involved in RNAi neutralization by HdIV. Indeed, some insect viruses have been shown to be able to prevent the destruction of viral RNAs by RNAi by expressing VSRs. For example, the binding of the viral protein VP3 from *Culex* Y virus (CYV) to viral dsRNAs and siRNAs prevents RNA recognition by the host Dicer-2 protein, thereby preventing the cleavage of dsRNAs into siRNAs (Fareh et al., 2018; van Cleef et al., 2014). DNA viruses also have VSR activity, as demonstrated by *Heliothis virescens* ascovirus (HvAV-3e), which encodes an RNAse III protein capable of inhibiting the host cell RNAi mechanism by degrading siRNAs (Hussain et al., 2010).

RNAi and the apoptotic pathway were downregulated in Sf9 cells challenged with HdIV. Both pathways are also targeted by baculoviruses (Ikeda et al., 2013; Karamipour et al., 2018), suggesting a similar mode of action for HdIV and baculoviruses. P35, a well-characterized apoptotic suppressor encoded by baculoviruses, has been shown to inhibit both these antiviral pathways, through different molecular mechanisms (Mehrabadi et al., 2015). However, no PDV protein has been found to share homology with P35, or with any other described viral inhibitor of apoptosis, such as IAP.

The induction of cell death in host cells playing a crucial role in immune defense would clearly be favorable for parasite development and, thus, for PDV, during parasitism. The activation of apoptosis may also contribute to the neutralization of the antiviral response, but in a different way, through its impact on RNAi. Indeed, the ectopic expression of apoptotic genes in different tissues has been shown to inhibit RNAi by blocking the processing of dsRNA into siRNA in *Drosophila melanogaster* (Xie et al., 2011). The analyses in various mutant laboratory strains have suggested that RNAi inhibition is caused by the adjacent apoptotic cells (Xie et al., 2011). If such a mechanism exists in PDV-infected lepidopteran hosts, then the combination of *dicer-2* downregulation and the inhibition of dsRNA processing may enhance the impairment of host antiviral defense by HdIV.

Our findings indicate also that other innate immune pathways are differentially regulated by HdIV. The Toll pathway was inhibited in Sf9 cells and fat bodies following HdIV challenge. Our findings were less clearcut for the IMD pathway, which was found to be inhibited in hemocytes, but activated in the fat body after HdIV infection. This finding may seem to go against the hypothesis of an inhibition of all antiviral pathways induced by viral infection in this tissue. However, in *Drosophila*, the overexpression of *imd, which* encodes a protein with a death domain, promotes apoptosis by inducing the transcription of pro-apoptotic genes (Georgel et al., 2001). The activation of the IMD pathway may therefore play an active role in inducing cell death in fat bodies infected with HdIV.

As the parasitized host remains alive for several days, coinfection or superinfection with another virus can occur in the field. Should this be the case, coinfection could alter the virulence properties of each virus, thereby compromising eventually the success of parasitism. Indeed, during the first 3–5 days after infection, JcDV-infected larvae died at higher levels relative to the coinfected larvae suggesting that HdIV enhances survival of *S. frugiperda* larvae to JcDV infection. JcDV is a non-enveloped virus, pathogenic for *Spodoptera* species fed on contaminated food or following intrahemocoelic injection (Mutuel et al., 2010; Vendeville et al., 2009). JcDV exhibits a rather broad tissue tropism in *S. frugiperda* larvae, including hemocytes, which are permissive for densovirus replication (Mutuel et al., 2010). Thus, apoptotic cell death induced by HdIV in hemocytes results in the elimination of several replicative niches for JcDV. However the densovirus is able to replicate in the non-apoptotic hemocytes and in other host tissues, such as the epidermis. Thus, inhibition of antiviral defense by HdIV could promote JcDV pathogenesis once the viral multiplication is sufficient to cause disease and death. This hypothesis may explain why, during the first phase of infection, we observed a delay in mortality in coinfected larvae compared with those observed for JcDV-infected larvae, while at a later stage, a slight increase in mortality is rather found in coinfected larvae than in JcDV-infected larvae.

In conclusion, our study reveals the complex interactions between HdIV and the immune antiviral defenses of the insect host, which depend on cell environment. This finding was not unexpected, as the objective of this particular virus is not to kill the host, but to neutralize and control host immune defense and development while keeping the host alive and relatively healthy for a few days. These results increase our understanding of the mechanism by which PDVs ensure successful parasitism.

Conflict of interest

The authors declare no financial or commercial conflict of interest.

Acknowledgements

We thank Clotilde Gibard and Gaetan Clabots for rearing the *S. frugiperda* larvae. We thank the quarantine insect platform (PIQ), member of the Vectopole Sud network, for providing the infrastructure needed for pest insect experimentations. We would like to thank Mylène Ogliastro and Cécile Clouet for providing the densovirus JcDV. We also thank Philippe Clair from qPHD platform (Montpellier GenomiX) for expert technical assistance with the real-time PCR experiments. We acknowledge the imaging facility MRI, member of the national infrastructure France-BioImaging supported by the French National Research Agency (ANR-10-INBS-04, «Investments for the future»). This work was supported by the division “Santé des Plantes et Environnement” of Institut National de la Recherche Agronomique.

References

Agaisse, H., Perrimon, N., 2004. The roles of JAK/STAT signaling in Drosophila immune responses. Immunol. Rev. 198, 72–82.
Avadhanula, V., Weasner, B.P., Hardy, G.G., Kumar, J.P., Hardy, R.W., 2009. A novel system for the launch of alphavirus RNA synthesis reveals a role for the Imd pathway in arthropod antiviral response. PLoS Pathog. 5 e1000582.
Beck, M.H., Zhang, S., Bitra, K., Burke, G.R., Strand, M.R., 2011. The encapsidated genome of Microplitis demolitor bracovirus integrates into the host Pseudoplusia includens. J. Virol. 85, 11685–11696.
Beliveau, C., Levasseur, A., Stoltz, D., Cusson, M., 2003. Three related TrIV genes: comparative sequence analysis and expression in host larvae and Cf-124T cells. J. Insect Physiol. 49, 501–511.
Beliveau, C., Cohen, A., Stewart, D., Periquet, G., Djoumad, A., Kuhn, L., Stoltz, D., Boyle, B., Volkoff, A.N., Herniou, E.A., et al., 2015. Genomic and proteomic analyses indicate that Banchine and campoplegine polydnaviruses have similar, if not identical, viral ancestors. J. Virol. 89, 8909–8921.
Bossin, H., Fournier, P., Royer, C., Barry, P., Cerutti, P., Gimenez, S., Couble, P., Bergoin, M., 2003. Junonia coenia densovirus-based vectors for stable transgene expression in Sf9 cells: influence of the densovirus sequences on genomic integration. J. Virol. 77, 11060–11071.
Brutscher, L.M., Daughenbaugh, K.F., Flenniken, M.L., 2015. Antiviral defense mechanisms in honey bees. Curr. Opin. Insect Sci. 10, 71–82.
Cai, M.J., Liu, W., He, H.J., Wang, J.X., Zhao, X.F., 2012. Mod(mdg4) participates in hormonally regulated midgut programmed cell death during metamorphosis. Apoptosis 17, 1327–1339.
Cao, X., He, Y., Hu, Y., Wang, Y., Chen, Y.R., Bryant, B., Clem, R.J., Schwartz, L.M., Blissard, G., Jiang, H., 2015. The immune signaling pathways of Manduca sexta. Insect Biochem. Mol. Biol. 62, 64–74.
Chevignon, G., Periquet, G., Gyapay, G., Vega-Czarny, N., Musset, K., Drezen, J.M., Huguet, E., 2018. Cotesia congregata bracovirus circles encoding PTP and ankyrin genes integrate into the DNA of parasitized Manduca sexta hemocytes. J. Virol. 92.
Choi, J.Y., Roh, J.Y., Wang, Y., Zhen, Z., Tao, X.Y., Lee, J.H., Liu, Q., Kim, J.S., Shin, S.W., Je, Y.H., 2012. Analysis of genes expression of Spodoptera exigua larvae upon AcMNPV infection. PLoS One 7 e42462.
Clavijo, G., Doremus, T., Ravallec, M., Mannucci, M.A., Jouan, V., Volkoff, A.N., Darboux, I., 2011. Multigenic families in Ichnovirus: a tissue and host specificity study through expression analysis of vankyrins from Hyposoter didymator Ichnovirus. PLoS One 6 e27522.
Clem, R.J., 2001. Baculoviruses and apoptosis: the good, the bad, and the ugly. Cell Death Differ. 8, 137–143.
Clem, R.J., 2016. Arboviruses and apoptosis: the role of cell death in determining vector competence. J. Gen. Virol. 97, 1033–1036.

Costa, A., Jan, E., Sarnow, P., Schneider, D., 2009. The Imd pathway is involved in antiviral immune responses in Drosophila. PLoS One 4, e7436.
DeWitte-Orr, S.J., Mehta, D.R., Collins, S.E., Suthar, M.S., Gale Jr., M., Mossman, K.L., 2009. Long double-stranded RNA induces an antiviral response independent of IFN regulatory factor 3, IFN-beta promoter stimulator 1, and IFN. J. Immunol. 183, 6545–6553.
Djoumad, A., Dallaire, F., Lucarotti, C.J., Cusson, M., 2013a. Characterization of the polydnaviral' T. Rostrale virus' (TrV) gene family: TrV1 expression inhibits in vitro cell proliferation. J. Gen. Virol. 94, 1134–1144.
Djoumad, A., Stoltz, D., Beliveau, C., Boyle, B., Kuhn, L., Cusson, M., 2013b. Ultrastructural and genomic characterization of a second banchine polydnavirus confirms the existence of shared features within this ichnovirus lineage. J. Gen. Virol. 94, 1888–1895.
Dong, S.M., Cui, J.H., Zhang, W., Zhang, X.W., Kou, T.C., Cai, Q.C., Xu, S., You, S., Yu, D.S., Ding, L., et al., 2017. Inhibition of translation initiation factor eIF4A is required for apoptosis mediated by Microplitis bicoloratus bracovirus. Arch. Insect Biochem. Physiol. 96.
Doremus, T., Cousserans, F., Gyapay, G., Jouan, V., Milano, P., Wajnberg, E., Darboux, I., Consoli, F.L., Volkoff, A.N., 2014. Extensive transcription analysis of the Hyposoter didymator Ichnovirus genome in permissive and non-permissive lepidopteran host species. PLoS One 9 e104072.
Dostert, C., Jouanguy, E., Irving, P., Troxler, L., Galiana-Arnoux, D., Hetru, C., Hoffmann, J.A., Imler, J.L., 2005. The Jak-STAT signaling pathway is required but not sufficient for the antiviral response of drosophila. Nat. Immunol. 6, 946–953.
Drezen, J.M., Leobold, M., Bezier, A., Huguet, E., Volkoff, A.N., Herniou, E.A., 2017. Endogenous viruses of parasitic wasps: variations on a common theme. Curr. Opin. Virol. 25, 41–48.
Dupuy, C., Gundersen-Rindal, D., Cusson, M., 2012. Genomics and replication of polydnaviruses. In: Beckage, N.E., Drezen, J.-M. (Eds.), Parasitoid Viruses: Symbionts and Pathogens. Academic Press, San Diego, pp. 47–61.
Estornes, Y., Toscano, F., Virard, F., Jacquemin, G., Pierrot, A., Vanbervliet, B., Bonnin, M., Lalaoui, N., Mercier-Gouy, P., Pacheco, Y., et al., 2012. dsRNA induces apoptosis through an atypical death complex associating TLR3 to caspase-8. Cell Death Differ. 19, 1482–1494.
Fareh, M., van Lopik, J., Katechis, I., Bronkhorst, A.W., Haagsma, A.C., van Rij, R.P., Joo, C., 2018. Viral suppressors of RNAi employ a rapid screening mode to discriminate viral RNA from cellular small RNA. Nucleic Acids Res. 46, 3187–3197.
Fath-Goodin, A., Kroemer, J.A., Webb, B.A., 2009. The Campoletis sonorensis ichnovirus vankyrin protein P-vank-1 inhibits apoptosis in insect Sf9 cells. Insect Mol. Biol. 18, 497–506.
Feng, G., Yu, Q., Hu, C., Wang, Y., Yuan, G., Chen, Q., Yang, K., Pang, Y., 2007. Apoptosis is induced in the haemolymph and fat body of Spodoptera exigua larvae upon oral inoculation with Spodoptera litura nucleopolyhedrovirus. J. Gen. Virol. 88, 2185–2193.
Ferreira, A.G., Naylor, H., Esteves, S.S., Pais, I.S., Martins, N.E., Teixeira, L., 2014. The Toll-dorsal pathway is required for resistance to viral oral infection in Drosophila. PLoS Pathog. 10 e1004507.
Flenniken, M.L., Andino, R., 2013. Non-specific dsRNA-mediated antiviral response in the honey bee. PLoS One 8 e77263.
Galiana-Arnoux, D., Dostert, C., Schneemann, A., Hoffmann, J.A., Imler, J.L., 2006. Essential function in vivo for Dicer-2 in host defense against RNA viruses in drosophila. Nat. Immunol. 7, 590–597.
Gammon, D.B., Mello, C.C., 2015. RNA interference-mediated antiviral defense in insects. Curr. Opin. Insect Sci. 8, 111–120.
Gantier, M.P., Williams, B.R., 2007. The response of mammalian cells to double-stranded RNA. Cytokine Growth Factor Rev. 18, 363–371.
Garbutt, J.S., Reynolds, S.E., 2012. Induction of RNA interference genes by double-stranded RNA; implications for susceptibility to RNA interference. Insect Biochem. Mol. Biol. 42, 621–628.
Georgel, P., Naitza, S., Kappler, C., Ferrandon, D., Zachary, D., Swimmer, C., Kopczynski, C., Duyk, G., Reichhart, J.M., Hoffmann, J.A., 2001. Drosophila immune deficiency (IMD) is a death domain protein that activates antibacterial defense and can promote apoptosis. Dev. Cell 1, 503–514.
Gundersen-Rindal, D.E., Lynn, D.E., 2003. Polydnavirus integration in lepidopteran host cells in vitro. J. Insect Physiol. 49, 453–462.
Hussain, M., Abraham, A.M., Asgari, S., 2010. An Ascovirus-encoded RNase III autoregulates its expression and suppresses RNA interference-mediated gene silencing. J. Virol. 84, 3624–3630.
Ikeda, M., Yamada, H., Hamajima, R., Kobayashi, M., 2013. Baculovirus genes modulating intracellular innate antiviral immunity of lepidopteran insect cells. Virology 435, 1–13.
Jacobs, B.L., Langland, J.O., 1996. When two strands are better than one: the mediators and modulators of the cellular responses to double-stranded RNA. Virology 219, 339–349.
Karamipour, N., Fathipour, Y., Talebi, A.A., Asgari, S., Mehrabadi, M., 2018. Small interfering RNA pathway contributes to antiviral immunity in Spodoptera frugiperda (Sf9) cells following Autographa californica multiple nucleopolyhedrovirus infection. Insect Biochem. Mol. Biol. 101, 24–31.
Kemp, C., Mueller, S., Goto, A., Barbier, V., Paro, S., Bonnay, F., Dostert, C., Troxler, L., Hetru, C., Meignin, C., et al., 2013. Broad RNA interference-mediated antiviral immunity and virus-specific inducible responses in Drosophila. J. Immunol. 190, 650–658.
Kim, M.K., Sisson, G., Stoltz, D., 1996. Ichnovirus infection of an established gypsy moth cell line. J. Gen. Virol. 77 (Pt 9), 2321–2328.
Kingsolver, M.B., Huang, Z., Hardy, R.W., 2013. Insect antiviral innate immunity: pathways, effectors, and connections. J. Mol. Biol. 425, 4921–4936.
Kroemer, J.A., Webb, B.A., 2006. Divergences in protein activity and cellular localization within the Campoletis sonorensis Ichnovirus Vankyrin family. J. Virol. 80, 12219–12228.
Kumarswamy, R., Chandna, S., 2010. Inhibition of microRNA-14 contributes to actinomycin-D-induced apoptosis in the Sf9 insect cell line. Cell Biol. Int. 34, 851–857.
Lapointe, R., Tanaka, K., Barney, W.E., Whitfield, J.B., Banks, J.C., Beliveau, C., Stoltz, D., Webb, B.A., Cusson, M., 2007. Genomic and morphological features of a banchine polydnavirus: comparison with bracoviruses and ichnoviruses. J. Virol. 81, 6491–6501.
Li, M., Pang, Z.Y., Xiao, W., Liu, X.Y., Zhang, Y., Yu, D.S., Yang, M.J., Yang, Y., Hu, J.S., Luo, K.J., 2014. A transcriptome analysis suggests apoptosis-related signaling pathways in hemocytes of Spodoptera litura after parasitization by microplitis bicoloratus. PLoS One 9.
Liu, W., Liu, J., Lu, Y., Gong, Y., Zhu, M., Chen, F., Liang, Z., Zhu, L., Kuang, S., Hu, X., et al., 2015. Immune signaling pathways activated in response to different pathogenic micro-organisms in Bombyx mori. Mol. Immunol. 65, 391–397.
Luo, K., Pang, Y., 2006. Spodoptera litura multicapsid nucleopolyhedrovirus inhibits Microplitis bicoloratus polydnavirus-induced host granulocytes apoptosis. J. Insect Physiol. 52, 795–806.
Marques, J.T., Imler, J.L., 2016. The diversity of insect antiviral immunity: insights from viruses. Curr. Opin. Microbiol. 32, 71–76.
McMenamin, A.J., Daughenbaugh, K.F., Parekh, F., Pizzorno, M.C., Flenniken, M.L., 2018. Honey bee and bumble bee antiviral defense. Viruses 10.
Mehrabadi, M., Hussain, M., Matindoost, L., Asgari, S., 2015. The baculovirus antiapoptotic p35 protein functions as an inhibitor of the host RNA interference antiviral response. J. Virol. 89, 8182–8192.
Miao, Y., Liang, A., Fu, Y., 2016. Baculovirus antiapoptotic protein P35 regulated the host apoptosis to enhance virus multiplication. Mol. Cell. Biochem. 423, 67–73.
Mutuel, D., Ravallec, M., Chabi, B., Multeau, C., Salmon, J.M., Fournier, P., Ogliastro, M., 2010. Pathogenesis of Junonia coenia densovirus in Spodoptera frugiperda: a route of infection that leads to hypoxia. Virology 403, 137–144.
Paradkar, P.N., Trinidad, L., Voysey, R., Duchemin, J.B., Walker, P.J., 2012. Secreted Vago restricts West Nile virus infection in Culex mosquito cells by activating the Jak-STAT pathway. Proc. Natl. Acad. Sci. U. S. A. 109, 18915–18920.
Poenisch, M., Burger, N., Staeheli, P., Bauer, G., Schneider, U., 2009. Protein X of Borna disease virus inhibits apoptosis and promotes viral persistence in the central nervous systems of newborn-infected rats. J. Virol. 83, 4297–4307.
Poitout, S., Bues, R., 1974. Linolenic acid requirements of lepidoptera Noctuidae Quadrifinae Plusiinae: Chrysodeixis chalcites Esp., Autographa gamma L.' Macdunnoughia confusa Stph., Trichoplusia ni Hbn. reared on artificial diets. Ann. Nutr. Aliment. 28, 173–187.
Provost, B., Jouan, V., Hilliou, F., Delobel, P., Bernardo, P., Ravallec, M., Cousserans, F., Wajnberg, E., Darboux, I., Fournier, P., et al., 2011. Lepidopteran transcriptome analysis following infection by phylogenetically unrelated polydnaviruses highlights differential and common responses. Insect Biochem. Mol. Biol. 41, 582–591.
Pruijssers, A.J., Falabella, P., Eum, J.H., Pennacchio, F., Brown, M.R., Strand, M.R., 2009. Infection by a symbiotic polydnavirus induces wasting and inhibits metamorphosis of the moth Pseudoplusia includens. J. Exp. Biol. 212, 2998–3006.
Robalino, J., Browdy, C.L., Prior, S., Metz, A., Parnell, P., Gross, P., Warr, G., 2004. Induction of antiviral immunity by double-stranded RNA in a marine invertebrate. J. Virol. 78, 10442–10448.
Salvia, R., Grossi, G., Amoresano, A., Scieuzo, C., Nardiello, M., Giangrande, C., Laurenzana, I., Ruggieri, V., Bufo, S.A., Vinson, S.B., et al., 2017. The multifunctional polydnavirus TnBVANK1 protein: impact on host apoptotic pathway. Sci. Rep. 7.
Souza-Neto, J.A., Sim, S., Dimopoulos, G., 2009. An evolutionary conserved function of the JAK-STAT pathway in anti-dengue defense. Proc. Natl. Acad. Sci. U. S. A. 106, 17841–17846.
Strand, M.R., Burke, G.R., 2012. Polydnaviruses as symbionts and gene delivery systems. PLoS Pathog. 8 e1002757.
Strand, M.R., Pech, L.L., 1995. Microplitis demolitor polydnavirus induces apoptosis of a specific haemocyte morphotype in Pseudoplusia includens. J. Gen. Virol. 76 (Pt 2), 283–291.
Suderman, R.J., Pruijssers, A.J., Strand, M.R., 2008. Protein tyrosine phosphatase-H2 from a polydnavirus induces apoptosis of insect cells. J. Gen. Virol. 89, 1411–1420.
Tanaka, K., Lapointe, R., Barney, W.E., Makkay, A.M., Stoltz, D., Cusson, M., Webb, B.A., 2007. Shared and species-specific features among ichnovirus genomes. Virology 363, 26–35.
van Cleef, K.W., van Mierlo, J.T., Miesen, P., Overheul, G.J., Fros, J.J., Schuster, S., Marklewitz, M., Pijlman, G.P., Junglen, S., van Rij, R.P., 2014. Mosquito and Drosophila entomobirnaviruses suppress dsRNA- and siRNA-induced RNAi. Nucleic Acids Res. 42, 8732–8744.
Vendeville, A., Ravallec, M., Jousset, F.X., Devise, M., Mutuel, D., Lopez-Ferber, M., Fournier, P., Dupressoir, T., Ogliastro, M., 2009. Densovirus infectious pathway requires clathrin-mediated endocytosis followed by trafficking to the nucleus. J. Virol. 83, 4678–4689.
Vilaplana, L., Pascual, N., Perera, N., Belles, X., 2007. Molecular characterization of an inhibitor of apoptosis in the Egyptian armyworm, Spodoptera littoralis, and midgut cell death during metamorphosis. Insect Biochem. Mol. Biol. 37, 1241–1248.
Volkoff, A.N., Rocher, J., Cerutti, P., Ohresser, M.C., d'Aubenton-Carafa, Y., Devauchelle, G., Duonor-Cerutti, M., 2001. Persistent expression of a newly characterized Hyposoter didymator polydnavirus gene in long-term infected lepidopteran cell lines. J. Gen. Virol. 82, 963–969.
Volkoff, A.N., Jouan, V., Urbach, S., Samain, S., Bergoin, M., Wincker, P., Demettre, E., Cousserans, F., Provost, B., Coulibaly, F., et al., 2010. Analysis of virion structural components reveals vestiges of the ancestral ichnovirus genome. PLoS Pathog. 6 e1000923.

Wang, P.H., Weng, S.P., He, J.G., 2015. Nucleic acid-induced antiviral immunity in invertebrates: an evolutionary perspective. Dev. Comp. Immunol. 48, 291–296.
Wang, Z.Z., Ye, X.Q., Shi, M., Li, F., Wang, Z.H., Zhou, Y.N., Gu, Q.J., Wu, X.T., Yin, C.L., Guo, D.H., et al., 2018. Parasitic insect-derived miRNAs modulate host development. Nat. Commun. 9, 2205.
Webb, B.A., Strand, M.R., Dickey, S.E., Beck, M.H., Hilgarth, R.S., Barney, W.E., Kadash, K., Kroemer, J.A., Lindstrom, K.G., Rattanadechakul, W., et al., 2006. Polydnavirus genomes reflect their dual roles as mutualists and pathogens. Virology 347, 160–174.
Weber, F., Wagner, V., Rasmussen, S.B., Hartmann, R., Paludan, S.R., 2006. Double-stranded RNA is produced by positive-strand RNA viruses and DNA viruses but not in detectable amounts by negative-strand RNA viruses. J. Virol. 80, 5059–5064.
Xi, Z., Ramirez, J.L., Dimopoulos, G., 2008. The Aedes aegypti toll pathway controls dengue virus infection. PLoS Pathog. 4 e1000098.
Xie, W., Liang, C., Birchler, J.A., 2011. Inhibition of RNA interference and modulation of transposable element expression by cell death in Drosophila. Genetics 188, 823–834.
Zambon, R.A., Nandakumar, M., Vakharia, V.N., Wu, L.P., 2005. The Toll pathway is important for an antiviral response in Drosophila. Proc. Natl. Acad. Sci. U. S. A. 102, 7257–7262.